

Geochronology of the Nabwal Hills: a record of earliest magmatism in the northern Kenyan Rift Valley

IAN McDOUGALL*‡ & RONALD T. WATKINS†

*Research School of Earth Sciences, The Australian National University, Canberra A.C.T. 0200, Australia

†Department of Applied Geology, Curtin University of Technology, PO Box U1987, Perth WA 6845, Australia

(Received 27 September 2004; accepted 12 May 2005)

Abstract – The Nabwal Hills, northeast of Lake Turkana, contain a record of magmatism associated with the initiation and early development of the East African Rift System in northernmost Kenya. The predominantly volcanic Asille Group, 1400 m thick, directly overlies metamorphic basement and comprises a sequence of basaltic lava flows with significant intervals of rhyolitic pyroclastic units, and minor intercalations of fluvial sediments. The basement gneisses yield K–Ar cooling ages on biotite of 510 and 522 Ma, typically Pan-African. The ^{40}Ar – ^{39}Ar ages on alkali feldspar crystals from the rhyolitic units are concordant and show that the Asille Group spans an interval from at least 34.3 to 15.8 Ma, continuing to at least as young as 13 Ma based on previous measurements. Vertebrate fossil sites, containing primate remains, at Irile and Nabwal are shown to be 17 ± 2 Ma old, Early Miocene, based upon K–Ar age measurements on immediately overlying basalts. Variably reliable whole rock K–Ar ages, determined on basalt samples from low in the sequence, indicate that volcanism commenced as early as 34.8 Ma ago. The overall geochronological results show that magmatism in the Nabwal Hills began about 35 Ma ago in Late Eocene times, interpreted as the time of initiation of crustal extension that led to the development of this segment of the East African Rift System. The Asille Group is tilted about 6° to the SSW. This tilting occurred later than 13 Ma ago, and prior to the eruption of the flat-lying Gombe Group basalts. These basalts may have begun erupting about 6 Ma ago in Late Miocene times, although much of this volcanism occurred between about 3.9 and 4.2 Ma ago in Pliocene times. It is suggested that the main rifting, which continues today, commenced in Late Miocene times, less than 13 Ma ago, and is partly reflected in the tilting of the Asille Group.

Keywords: basalts, ignimbrites, geochronology, Kenya, tectonics.

1. Introduction

The Nabwal Hills are located in the extremely remote eastern portion of the Suregei-Asille uplands, a horst-like structure lying between the Lake Turkana and Chew Bahir (formerly Lake Stefanie) rift basins in northernmost Kenya and southern Ethiopia (Fig. 1). This same horst block, forming the margin of the Chew Bahir Rift, extends northwards some 100 km into southern Ethiopia, where it is known as the Hamar Horst (Moore & Davidson, 1978) (Fig. 1). The Nabwal Hills rise a few hundred metres above the floor of Chew Bahir, immediately to the east, and Lake Turkana, to the west, reaching an altitude of 900 m.

The Kenya Rift bifurcates just south of Lake Turkana with one branch extending NNE through the Kinu Sogo fault zone to the Chew Bahir Rift, and the other branch aligned due north through Lake Turkana and into the Omo Valley of southern Ethiopia (Moore & Davidson, 1978; Davidson, 1983; Key & Watkins, 1988). The Nabwal Hills horst lies between these two rift branches in a segment of the East African Rift System between the Ethiopian and East African domes (Fig. 1). Here

the broad system of faulting is as much as 300 km wide, as opposed to less than 100 km wide elsewhere along the rift (Morley *et al.* 1999; Ebinger *et al.* 2000). This region includes both the oldest volcanics (Eocene) and oldest rift basins (Oligocene) in the East African Rift System and is a key to understanding the early structural and volcanic evolution of the rift.

The rift in the Turkana region of northern Kenya has more subdued relief than where the rift transects the elevated domes to the north and south. Lithological evidence of early rift evolution in this region is largely obscured beneath extensive floods of relatively young basalts as well as lacustrine and fluviodeltaic sediments of the Turkana Basin. The Suregei-Asille uplands provide a rare opportunity to observe the underlying rocks, including exposures of basement gneisses in the Nabwal Hills. This metamorphic basement is overlain unconformably by a sequence of volcanic and lesser sedimentary strata some 1400 metres thick, the Asille Group (R. T. Watkins, unpub. Ph.D. thesis, Univ. London, 1983; Key & Watkins, 1988). These strata exhibit a regional dip of $\sim 6^\circ$ to the SSW, and are overlain by essentially flat-lying basaltic lavas of the Gombe Group up to 200 m thick (Watkins, 1986; Haileab *et al.* 2004). To the west and southwest lie

‡ Author for correspondence: Ian.McDougall@anu.edu.au

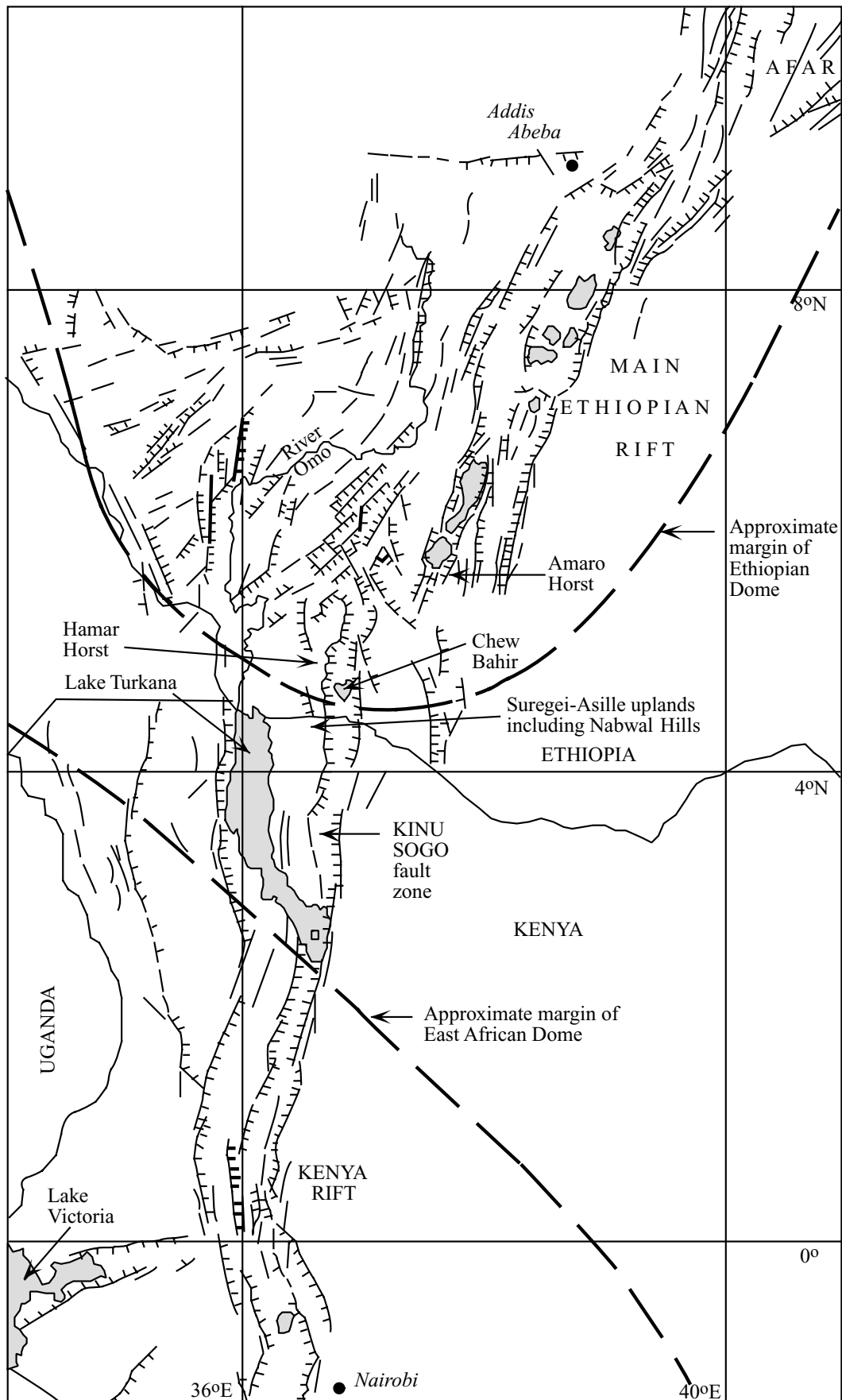


Figure 1. Regional tectonic map of the East African Rift system, modified after Davidson (1983), Ebinger *et al.* (1989) and Morley, Ngenoh & Ego (1999).

sediments of the Turkana Basin renowned for their hominid fossils, with deposition commencing about 4.2 Ma ago (Leakey *et al.* 1998; McDougall & Feibel, 1999).

The geology of the major part of the Suregei-Asille uplands was mapped in detail by R. T. Watkins (unpub. Ph.D. thesis, Univ. London, 1983). At that time, study of the easternmost part, the Nabwal Hills, was limited to a single transect extending across-strike from the outcrop of metamorphic basement. Detailed investigation of the lowest part of the volcanic sequence in this area took place in 1999. Other geological expeditions to the Nabwal Hills have led to the discovery of two new vertebrate fossil localities, bearing remains of primates (Fleagle *et al.* 1997, 2000) within fluvial sediments intercalated with the volcanic strata, prompting additional interest in the age of the sequence.

Rift faulting and voluminous volcanism are characteristics of the East African Rift System in Kenya and Ethiopia, but there remains much conjecture over the relative timing of their inception, as well as over the timing and direction of propagation of both the faulting and volcanism. Elucidation of such spatial trends requires precise dating of the sequences, the main aim of the present study of the Asille Group volcanics. The Asille Group is bimodal, dominated by basaltic rocks, but with several episodes of rhyolitic pyroclastic eruption that are laterally extensive, providing invaluable stratigraphic markers in the heavily faulted succession.

Here we present results of K–Ar and ^{40}Ar – ^{39}Ar age determinations undertaken on samples collected during the expeditions to the Nabwal Hills to enhance the numerical age control of the Asille Group. Age determinations on a welded rhyolitic ignimbrite and basaltic lavas have extended the detailed record to the lowermost part of the succession, the Nabwal Formation, and provide an age for the initiation of this segment of the East African Rift System. Additional ^{40}Ar – ^{39}Ar ages on alkali feldspars from other important rhyolitic markers confirm and refine their ages. K–Ar age measurements on basalt lavas provide estimates for the age of the recently discovered fossil sites.

2. Regional geological setting

Geophysical evidence, especially seismic data, shows that in the Turkana region, crustal extension amounts to about 40 km across the rift (Morley *et al.* 1992; Hendrie *et al.* 1994; Morley, Ngenoh & Ego, 1999), with significant thinning of the crust to about 20 km essentially under Lake Turkana (KRISP, 1991; Mechie *et al.* 1994). Detailed seismic information acquired by Amoco and Shell (Morley *et al.* 1992; Morley, 1999) immediately to the west of Lake Turkana reveals the presence of extensive N–S-trending half grabens filled with as much as 7 km of fluviodeltaic sands and lacustrine shales, together with significant volumes of basaltic volcanics in the upper part of the section.

Exploration wells drilled by Shell to a depth of nearly 3 km in the Lokichar Basin and the Kerio Basin have assisted in interpretation of the seismic data (Morley *et al.* 1999), demonstrating that the oldest fill in the Lokichar Basin is of early Oligocene to possibly Eocene age and indicating that major extension and basin subsidence was already occurring at this time.

From gravity and topographic data, Ebinger *et al.* (1989) showed that the Ethiopian Dome and the East African Dome (Fig. 1), transected by the relatively narrow rift system, are best explained by dynamic uplift above a convecting region within the asthenospheric mantle, and that this has caused significant heating and thinning of the lithosphere. Such an interpretation, taken together with the widespread flood basalt volcanism associated with the rift system and the domes, gave rise to the idea that hot mantle plumes exist in the mantle beneath the region, with the Afar plume underlying the Ethiopian Dome and a separate plume lying below the East African Dome (Ebinger *et al.* 1993), noting that Mohr (1983) had earlier suggested the presence of such a plume beneath the Ethiopian Dome. Strong support for the plume concept arose from the recognition that the amount of crustal extension associated with the rifting, generally less than 40 km, was insufficient for the simple adiabatic decompression mantle melting model of McKenzie & Bickle (1988) to have accounted for the observed voluminous flood basalts (Latin, Norry & Tarzey, 1993; Ebinger *et al.* 1993; Hendrie *et al.* 1994). As a result, the idea of hot upwelling mantle under the domes in the form of a mantle plume or plumes, possibly as a major causative factor in the volcanism and rifting, has become widely accepted.

An area that has been rather extensively studied is the Amaro Horst block within the Main Ethiopian Rift, near its southern termination, about 120 km NNE of the Nabwal Hills (Fig. 1). There are some similarities between the two areas, as will be discussed later. At Amaro, metamorphic basement crops out, overlain by basaltic lavas long recognized to represent two distinct magmatic phases occurring 45 to 35 Ma ago and 19 to 11 Ma ago (WoldeGabriel *et al.* 1991; Ebinger *et al.* 1993). George, Rogers & Kelley (1998) provided further confirmation of the age of these magmatic phases, and suggested that the earliest phase was initiated above the Kenyan (East African) plume and the younger volcanism was associated with the Afar plume as the African (Nubian) plate migrated NE over the plumes at a rate similar to the 25 mm a⁻¹ measured at the present time (Fernandes *et al.* 2004) and also over longer time scales (DeMets *et al.* 1990, 1994; Chu & Gordon, 1999).

Detailed geochemical studies of Eocene to Recent basalts associated with the rifts in southern Ethiopia and northern Kenya have sought to distinguish their possible lithospheric and asthenospheric mantle sources (Latin, Norry & Tarzey, 1993; Stewart &

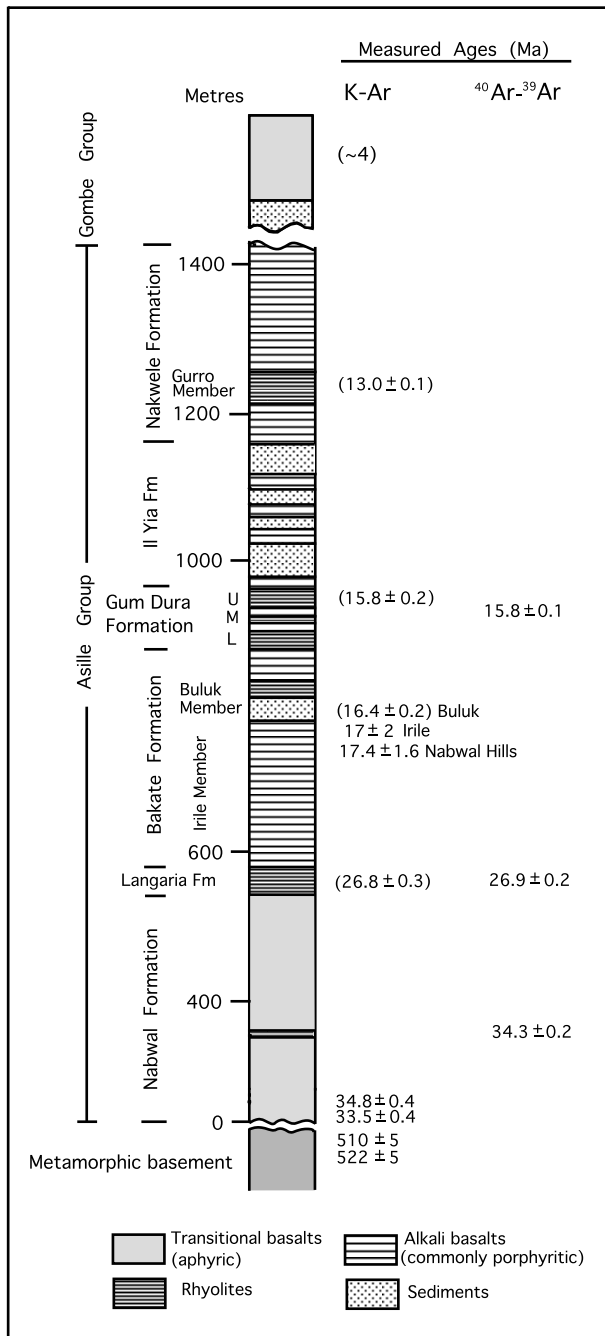


Figure 2. Schematic stratigraphy of the Asille Group, with ages indicated. Ages in parentheses are from earlier publications; see text.

Rogers, 1996; Rogers *et al.* 2000; Macdonald *et al.* 2001; George & Rogers, 2002; Furman *et al.* 2004), although as noted by Macdonald, Williams & Gass (1994), the geochemical evidence often remains equivocal.

3. Previous geochronological studies

The stratigraphy of the Asille Group has been summarized in several publications (e.g. Fitch *et al.* 1985; McDougall & Watkins, 1988; Key & Watkins, 1988) and is shown schematically in Figure 2. Previous re-

gional geochronological studies were presented by Fitch *et al.* (1985) and McDougall & Watkins (1988). A K–Ar age of 28.2 ± 0.7 Ma on a basalt lava collected from the initial reconnaissance transect from near the base of the Nabwal Formation provided the previous best estimate of the beginning of volcanism in the region (Fitch *et al.* 1985). McDougall & Watkins (1988) obtained consistent K–Ar ages on alkali feldspar from four samples from three pantelleritic ignimbrites of the stratigraphically higher Langaria Formation averaging 26.8 ± 0.3 Ma. McDougall & Watkins (1985) reported good K–Ar age control of 16.2 to 17.2 Ma for part of the Bakate Formation, and 15.8 ± 0.2 Ma for distinctive welded ignimbrites in the overlying Gum Dura Formation. Potassium–argon ages of 13.0 ± 0.1 Ma on alkali feldspar from the Gurro Member of the Nakwele Formation (McDougall & Watkins, 1988) provided age control for the younger part of the Asille Group.

4. Methods and techniques

Samples were collected from the Nabwal Hills with the aim of providing as good a time framework as possible for the lower part of the Asille Group. The location of most samples is shown on Figure 3. Each was examined in petrographic thin-section for suitability for dating by the K–Ar and ^{40}Ar – ^{39}Ar techniques. Basalt lavas of the Nabwal Formation from low in the succession were nearly aphyric, consisting of unaltered plagioclase, clinopyroxene and minor olivine and iron oxide, with relatively abundant (up to ~15%) intersertal glass, showing varying degrees of devitrification and alteration. Only the least altered samples were selected for dating, but petrographic examination alone provides a somewhat subjective approach to ensuring that the results accurately reflect crystallization ages. Basalts from the Irile Member, Bakate Formation, most commonly are strongly porphyritic in plagioclase with less common olivine, set in a distinctive subophitic groundmass of large clinopyroxene crystals and plagioclase laths, together with olivine, Fe–Ti oxides, and up to 20% of glassy mesostasis, variably crystallized. In some cases we separated plagioclase for K–Ar age determinations as well as measuring whole rock samples.

The rhyolites commonly contain phenocrysts of alkali feldspar that are limpid and unaltered. Alkali feldspar was separated in each case, and age measurements made by the ^{40}Ar – ^{39}Ar technique, using both the single crystal total fusion approach and step heating of aggregates of crystals to produce age spectra. Single crystals were fused in the ultrahigh vacuum system by means of a continuous wave laser beam (argon ion), following irradiation of the samples with fast neutrons in a nuclear reactor. The step heating measurements were made by utilizing a double vacuum resistance heating furnace for the controlled release of argon

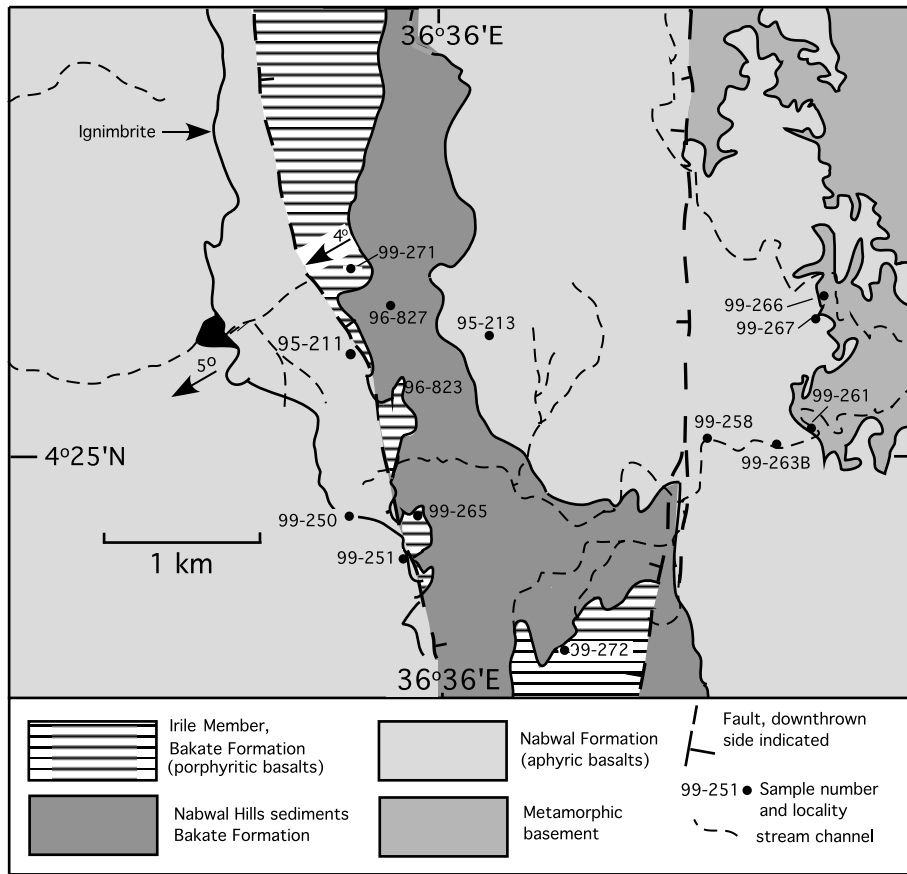


Figure 3. Simplified geological map of the Nabwal Hills site, northern Kenya, immediately south of the Ethiopian border. Based on mapping by R. T. Watkins. Localities of dated samples are shown. Base map is not well controlled.

with increasing temperature. The procedures used have been described by McDougall & Feibel (1999). All isotopic measurements of argon were performed in a VG3600 gas-source mass spectrometer with a Daly detector operating at a sensitivity of approximately $5 \times 10^{-17} \text{ mol mV}^{-1}$. The fluence monitor employed in the ^{40}Ar - ^{39}Ar measurements was sanidine 92-176 separated from the Fish Canyon Tuff (Colorado) with a reference K–Ar age of 28.1 Ma (Spell & McDougall, 2003). Correction factors for calcium interferences were those listed in Spell, McDougall & Doulgeris (1996) and McDougall & Harrison (1999), whereas the $(^{40}\text{Ar}/^{39}\text{Ar})_{\text{K}}$ correction factor was determined in each irradiation and ranged from 0.0246 to 0.0262. Fast neutron irradiations were performed in facility X33 or X34 of HIFAR reactor, Lucas Heights, New South Wales, for 144 h, with inversion of the reactor canister at regular intervals to ensure that the fast neutron flux gradient was minimized.

The K–Ar measurements were made by methods similar to those described by McDougall & Feibel (1999). Potassium was determined by flame photometry and the argon by isotope dilution utilizing a ^{38}Ar tracer. Uncertainties in the K–Ar ages averaged about 1 % standard deviation. Decay constants utilized were those recommended by Steiger & Jäger (1977).

The numerical time scale used in this study is that proposed by Berggren *et al.* (1995) in which the Eocene–Oligocene, Oligocene–Miocene, Miocene–Pliocene and Pliocene–Quaternary boundaries have estimated ages of 33.7, 23.8, 5.3 and 1.77 Ma, respectively. All geographic coordinates are from GPS observations using WGS 84 as the datum.

5. Results and discussion

K–Ar data are listed in Table 1, ^{40}Ar - ^{39}Ar results are given in Tables 2 to 5, and the best estimates of age are shown in Figure 2.

5.a. Basement rocks

Exposures of metamorphic rocks in the northeastern part of the Nabwal Hills represent the only outcrop of metamorphic basement to be found on the eastern side of the Lake Turkana graben. They comprise gneisses and schists with northerly-trending foliation dipping about 50° to the west. Biotite was separated from two gneisses from outcrops about 2 km apart in the Nabwal Hills (Fig. 3). Measured K–Ar ages of 510 ± 5 and 522 ± 5 Ma (Table 1) are quite typical of the Mozambique Belt, rocks of which are widespread

Table 1. Potassium-argon ages on biotite from basement gneisses, on whole rock nearly aphyric basalts from the Nabwal Formation, and from feldsparphyric basalts of the Irile Member of the Bakate Formation, Nabwal Hills, northern Kenya

Sample number	Material	K wt %	⁴⁰ Ar* 10 ⁻¹¹ mol g ⁻¹	% ⁴⁰ Ar*	Calculated age Ma ± 1 s.d.	Latitude N	Longitude E	Locality
<i>Irile Member basalts overlying sediments in the Nabwal Hills</i>								
99-271	Whole rock	1.050, 1.052	3.246	25.2	17.7 ± 0.2	4°25.81'	36°35.60'	Overlying sediments, near monkey site
"	"	"	3.322	33.5	18.1 ± 0.2	"	"	"
99-271	Plagioclase	0.194, 0.195	0.564	45.2	16.7 ± 0.2	"	"	"
96-823	Plagioclase	0.198, 0.198	0.599	19.8	17.4 ± 0.3	4°25.32'	36°35.80'	Overlying sediments at rhinoceros site
99-265	Whole rock	0.947, 0.937	3.377	37.5	20.6 ± 0.2	4°24.72'	36°35.96'	Overlying sediments, proboscidean site
99-265	Plagioclase	0.195, 0.200	0.581	39.0	16.9 ± 0.3	"	"	"
99-272	Whole rock	1.046, 1.048	2.917	78.1	16.0 ± 0.2	4°24.07'	36°36.67'	Overlying sediments, southern limit
99-272	Plagioclase	0.203, 0.200	0.566	40.4	16.2 ± 0.3	"	"	"
<i>Irile Member basalts overlying sediments at Irile site</i>								
99-268	Whole rock	0.597, 0.597	1.574	56.6	15.1 ± 0.2	4°22.04'	36°33.69'	About third flow above sediments
99-268	Plagioclase	0.152, 0.153	0.523	22.8	19.7 ± 0.3	"	"	"
99-269	Whole rock	0.715, 0.720	2.145	39.2	17.2 ± 0.2	4°22.09'	36°33.69'	About second flow above sediments
99-269	Plagioclase	0.162, 0.162	0.466	61.4	16.5 ± 0.2	"	"	"
<i>Nabwal Formation, aphyric basalt lava flows</i>								
95-211	Whole rock	0.768, 0.766	4.032	39.7	30.1 ± 0.3	4°25.47'	36°35.53'	Just W of sediments, across fault (95-6-K)
96-827	Whole rock	0.754, 0.743	3.906	23.2	29.8 ± 0.6	4°25.70'	36°35.69'	Flow, adjacent to monkey site (KNH-96-5)
95-213	Whole rock	1.020, 1.043	5.530	66.2	30.7 ± 0.7	4°25.54'	36°36.17'	Flow, below and east of sediments (95-8-K)
99-258	Whole rock	0.891, 0.887	4.292	69.8	27.6 ± 0.3	4°25.41'	36°37.14'	Flow, close to basement
99-263B	Whole rock	0.469, 0.470	2.862	59.3	34.8 ± 0.4	4°25.18'	36°37.45'	Thick (~20 m+) flow, close to basement
99-267	Whole rock	0.818, 0.823	4.809	81.7	33.5 ± 0.4	4°26.12'	36°37.50'	Overlying basement gneiss
<i>Biotite gneisses of local basement</i>								
99-266	Biotite	7.83, 7.78	798.7	99.1	510.4 ± 5.3	4°26.16'	36°37.49'	From river courses draining southeast
99-261	Biotite	7.68, 7.73	809.1	89.4	522.1 ± 5.4	4°25.27'	36°37.85'	from Nabwal Hills toward Chew Bahir

$\lambda_c = 0.581 \times 10^{-10} \text{ a}^{-1}$; $\lambda_\beta = 4.962 \times 10^{-10} \text{ a}^{-1}$; $^{40}\text{K}/\text{K} = 1.167 \times 10^{-4} \text{ mol/mol}$.
⁴⁰Ar* = radiogenic argon; Datum: WGS 84.

in Africa and generally reflect so-called Pan-African events (Cahen & Snelling, 1966). These Early Palaeozoic ages most likely record the time of cooling of the biotite through its closure temperature for argon retention, and thus relate to uplift and exhumation of the terrane rather than the time of biotite formation during metamorphism.

5.b. Asille Group volcanics

The bimodal sequence of mainly basaltic lavas, with rhyolitic pyroclastic rocks occurring at intervals, is typical of the Turkana region. We had difficulty in obtaining consistent results from the basalt lavas. However, we believe that the ages measured on alkali feldspar from three rhyolitic intercalations within the Asille Group are not only precise but provide an accurate record of the time of eruption. As the ages on the alkali feldspars provide key time constraints for the Asille Group, these results will be presented first, followed by discussion of the K–Ar apparent ages of the basaltic rocks.

5.b.1. Rhyolites

The first occurrence of rhyolitic volcanics crops out in the upper half of the Nabwal Formation, approximately 300 m from the base (Fig. 3). The rhyolite has the form of a variably welded and massive, crystal-rich ignimbrite and associated non-welded pyroclastic deposits. Despite a maximum thickness of less than

5 m, the unit can be traced intermittently across the Nabwal Hills. The ignimbrite was sampled at two outcrops approximately 600 m apart (Fig. 3), and the feldspars separated. Results of total fusion ⁴⁰Ar–³⁹Ar age measurements on single crystals, averaging about 0.1 mg, are given in Table 2. Eleven crystals were measured for sample 99-250. The ages obtained are remarkably concordant, yielding an arithmetic mean of $34.18 \pm 0.23 \text{ Ma}$, where the quoted uncertainty is the standard deviation of the population. Similarly, for sample 99-251, from which nine crystals were separately fused and analysed, a concordant set of ages was obtained with arithmetic mean of $34.31 \pm 0.19 \text{ Ma}$. These two sets of ages are in agreement. The combined probability plot (Fig. 4), although not perfectly Gaussian, shows that we are dealing with an essentially homogeneous age group, interpreted as a juvenile volcanic population.

Multigrained samples of the two alkali feldspar separates were step heated (Table 3); age spectra produced in these experiments are shown in Figure 5. Both feldspar samples yield nearly flat age spectra, with an initial (low-temperature) step or two having slightly higher apparent ages, and step 16 of 99-250 showing a lower age. The weighted mean plateau ages are similar to one another at 34.28 ± 0.18 and $34.47 \pm 0.17 \text{ Ma}$ for 99-250 and 99-251, respectively, where the quoted errors include the uncertainty of 0.5 % in the irradiation parameter, J. The flat, near-ideal age spectra indicate that these feldspars have remained undisturbed thermally since cooling after eruption. Similar ages

Table 2. Results of laser fusion ^{40}Ar - ^{39}Ar dating of single crystals of alkali feldspar from two samples of ignimbrite, a unit about 1 m thick interbedded with basalts of the Nabwal Formation, Nabwal Hills, northern Kenya

Crystal no.	$^{36}\text{Ar}/^{39}\text{Ar} \times 10^{-4}$	$^{37}\text{Ar}/^{39}\text{Ar} \times 10^{-3}$	$^{40}\text{Ar}/^{39}\text{Ar}$	$^{40}\text{Ar}^*/^{39}\text{Ar}_K \pm \text{c.v.}$	% $^{40}\text{Ar}^*$	$^{39}\text{Ar} 10^{-15} \text{ mol}$	Calculated age Ma $\pm 1 \text{ s.d.}$
99-250, ignimbrite, $4^\circ 24.84' \text{N}$, $36^\circ 35.46' \text{E}$; $J = 3.869\text{E-}03 \pm 0.50\%$; level 4, ANU59							
1	0.314	4.587	5.011	$4.977 \pm 0.35\%$	99.3	7.5	34.41 ± 0.21
2	1.734	0.291	5.045	$4.969 \pm 0.26\%$	98.5	6.7	34.36 ± 0.19
3	8.742	0.166	5.275	$4.992 \pm 0.70\%$	94.6	5.1	34.52 ± 0.29
4	1.736	2.196	5.004	$4.928 \pm 0.30\%$	98.5	4.7	34.07 ± 0.20
5	0.388	0.165	5.007	$4.970 \pm 0.36\%$	99.3	5.1	34.37 ± 0.21
6	43.426	1.544	6.270	$4.962 \pm 0.47\%$	79.1	7.8	34.31 ± 0.23
7	1.769	0.136	4.996	$4.919 \pm 0.25\%$	98.5	6.2	34.02 ± 0.19
8	2.657	3.394	5.049	$4.946 \pm 0.36\%$	98.0	3.6	34.20 ± 0.21
9	3.510	0.651	5.057	$4.929 \pm 0.36\%$	97.5	4.5	34.08 ± 0.21
10	4.621	10.590	5.060	$4.899 \pm 0.59\%$	96.8	4.6	33.88 ± 0.26
11	3.415	7.442	5.016	$4.891 \pm 0.50\%$	97.5	5.2	33.82 ± 0.24
Arithmetic mean age (n = 11)							34.18 ± 0.23
99-251, ignimbrite, $4^\circ 24.71' \text{N}$, $36^\circ 35.79' \text{E}$; $J = 3.950\text{E-}03 \pm 0.50\%$; level 6, ANU59							
2	0.700	3.316	4.944	$4.898 \pm 0.65\%$	99.1	3.9	34.57 ± 0.28
3	1.899	25.059	4.899	$4.820 \pm 0.50\%$	98.4	2.7	34.02 ± 0.24
4	2.311	2.997	4.933	$4.839 \pm 0.31\%$	98.1	5.7	34.16 ± 0.20
5	1.939	16.494	4.955	$4.874 \pm 0.39\%$	98.4	3.5	34.40 ± 0.22
6	2.404	24.656	4.945	$4.851 \pm 0.39\%$	98.1	2.4	34.24 ± 0.22
7	1.664	5.239	4.964	$4.889 \pm 0.62\%$	98.5	3.4	34.51 ± 0.27
8	1.658	0.201	4.945	$4.870 \pm 0.31\%$	98.5	4.4	34.38 ± 0.20
9	1.435	4.936	4.949	$4.881 \pm 0.29\%$	98.6	6.4	34.46 ± 0.20
10	3.950	9.248	4.970	$4.829 \pm 0.30\%$	97.2	4.4	34.09 ± 0.20
Arithmetic mean age (n = 9)							34.31 ± 0.19

$\lambda = 5.543 \times 10^{-10} \text{ a}^{-1}$; sensitivity $\sim 2.6 \times 10^{17} \text{ mol mV}^{-1}$.
 $(^{36}\text{Ar}/^{37}\text{Ar})_{\text{Ca}} = 3.50 \times 10^{-4}$; $(^{39}\text{Ar}/^{37}\text{Ar})_{\text{Ca}} = 7.86 \times 10^{-4}$; $(^{40}\text{Ar}/^{39}\text{Ar})_{\text{K}} = 0.0249$ (99-250), 0.0257 (99-251).
 $^{40}\text{Ar}^*$ – radiogenic ^{40}Ar ; $^{39}\text{Ar}_K$ – K-derived ^{39}Ar ; quoted error for each age includes estimated error in J.
 Irradiation for 144 hours in X33 or X34, HIFAR reactor.
 Fluence monitor: 92-176 sanidine from Fish Canyon Tuff; K-Ar reference age: 28.1 Ma.

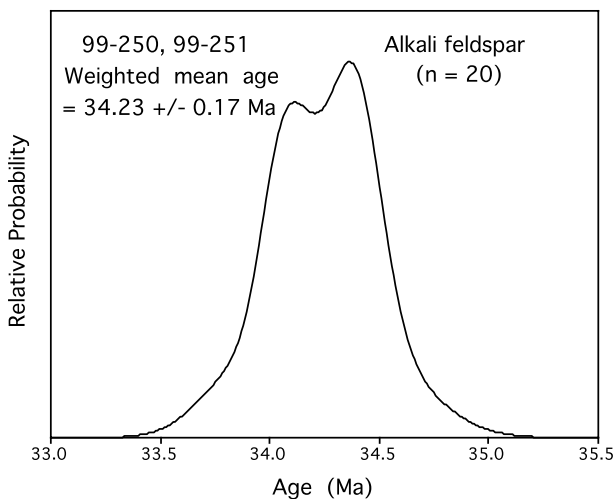


Figure 4. Probability plot of total fusion age data from single crystals of alkali feldspar from two samples (99-250 and 99-251) of the same ignimbrite, Nabwal Formation.

are derived from isotope correlation plots of the step heating data (Table 3). Overall, the results from single crystal total fusion measurements, together with the age spectra, provide unequivocal evidence for an age of $34.3 \pm 0.2 \text{ Ma}$ for this rhyolitic unit, Late Eocene in terms of the time scale of Berggren *et al.* (1995).

The Langaria Formation is the second, and far more voluminous, manifestation of rhyolitic (pantelleritic)

volcanism recorded in the Asille Group succession. At the type location of Langaria Cliffs on the Il Jimma River ($4^\circ 26.79' \text{N}$, $36^\circ 24.98' \text{E}$) a 35.6 m thick sequence includes four prominent, massively welded ignimbrite units. Alkali feldspars from three of these units have yielded concordant K–Ar ages of $26.8 \pm 0.3 \text{ Ma}$ (McDougall & Watkins, 1988). During the present study, a further sample of ignimbrite was collected from a prominent bluff in the Irile Valley on the southwestern margin of the Nabwal Hills. Here a distinctive pink-coloured welded ignimbrite, about 10 m thick, caps the rhyolitic sequence, and has a similar appearance to the youngest ignimbrite seen at the type locality in the Langaria Cliffs, some 17 km to the WNW. The unit demonstrably overlies the basalt lavas of the Nabwal Formation, and underlies the Irile Member of the Bakate Formation (R. T. Watkins, unpub. Ph.D. thesis, Univ. London, 1983). Alkali feldspar from the ignimbrite sample (99-270) yielded concordant ^{40}Ar - ^{39}Ar total fusion ages on 14 single crystals, with an overall mean of $26.86 \pm 0.17 \text{ Ma}$ (Table 4), reflecting an essentially homogeneous population (see probability plot, Fig. 6). The age spectrum derived from a step heating experiment on a multigrained feldspar aliquot of the same mineral separate (Table 5, Fig. 7) shows that the two initial steps yield quite high apparent ages, but that for 95 % of the argon released in the 15 higher temperature steps, the age spectrum is ideally flat, giving a weighted

Table 3. Results of ^{40}Ar – ^{39}Ar step heating experiments on alkali feldspar separated from ignimbrite interbedded with basalts of the Nabwal Formation, Nabwal Hills, northern Kenya, $4^{\circ}24.65'\text{N}$, $36^{\circ}35.51'\text{E}$ (99-250) and $4^{\circ}24.52'\text{N}$, $36^{\circ}35.84'\text{E}$ (99-251)

Step no.	Temp. °C	$^{36}\text{Ar}/^{39}\text{Ar}$ $\times 10^{-3}$	$^{37}\text{Ar}/^{39}\text{Ar}$ $\times 10^{-3}$	$^{40}\text{Ar}/^{39}\text{Ar}$	$^{40}\text{Ar}^*/^{39}\text{Ar}_K$ \pm c.v.	% $^{40}\text{Ar}^*$	^{39}Ar 10^{-14} mol	Calculated age Ma \pm 1 s.d.
<i>99-250 alkali feldspar, $J = 3.869\text{E-}03 \pm 0.5\%$; level 4, ANU59, 4.2 mg</i>								
1	700	9.608	32.335	8.090	$5.229 \pm 1.66\%$	64.6	0.23	36.14 ± 0.62
2	800	3.607	14.506	6.143	$5.054 \pm 0.63\%$	82.3	0.63	34.94 ± 0.28
3	900	1.862	3.226	5.573	$4.999 \pm 0.23\%$	89.7	1.60	34.56 ± 0.19
4	950	2.047	3.582	5.591	$4.961 \pm 0.34\%$	88.7	1.72	34.30 ± 0.21
5	990	2.113	7.579	5.626	$4.978 \pm 0.28\%$	88.5	1.86	34.42 ± 0.19
6	1020	2.439	3.030	5.715	$4.970 \pm 0.30\%$	87.0	1.84	34.36 ± 0.20
7	1050	2.708	4.783	5.786	$4.962 \pm 0.22\%$	85.7	1.92	34.31 ± 0.19
8	1080	3.065	3.847	5.877	$4.947 \pm 0.22\%$	84.2	2.00	34.20 ± 0.18
9	1100	3.701	–	6.048	$4.930 \pm 0.41\%$	81.5	1.82	34.09 ± 0.22
10	1120	3.856	8.820	6.107	$4.944 \pm 0.29\%$	81.0	1.75	34.19 ± 0.20
11	1140	3.437	1.552	5.976	$4.936 \pm 0.29\%$	82.6	1.75	34.13 ± 0.19
12	1160	3.930	–	6.121	$4.935 \pm 0.37\%$	80.6	1.73	34.12 ± 0.21
13	1180	4.801	13.262	6.378	$4.936 \pm 0.38\%$	77.4	1.59	34.13 ± 0.21
14	1210	5.767	–	6.682	$4.953 \pm 0.39\%$	74.1	1.53	34.25 ± 0.22
15	1250	10.046	8.800	7.955	$4.963 \pm 0.68\%$	62.4	1.13	34.32 ± 0.29
16	1300	39.299	19.995	16.466	$4.831 \pm 1.85\%$	29.4	0.42	33.41 ± 0.64
<i>99-251 alkali feldspar, $J = 3.950\text{E-}03 \pm 0.5\%$; level 6, ANU59, 4.0 mg</i>								
1	750	3.470	2.570	6.143	$5.092 \pm 0.90\%$	82.9	0.63	35.93 ± 0.36
2	850	1.082	2.456	5.244	$4.899 \pm 0.14\%$	93.4	1.42	34.58 ± 0.18
3	920	0.627	7.877	5.092	$4.822 \pm 0.18\%$	95.9	2.67	34.46 ± 0.18
4	960	0.677	0.982	5.100	$4.874 \pm 0.14\%$	95.6	2.65	34.40 ± 0.18
5	980	0.807	3.932	5.169	$4.905 \pm 0.21\%$	94.9	2.11	34.62 ± 0.19
6	1000	1.022	4.326	5.201	$4.874 \pm 0.27\%$	93.7	1.92	34.40 ± 0.19
7	1020	1.184	5.603	5.243	$4.868 \pm 0.24\%$	92.8	1.80	34.36 ± 0.19
8	1040	1.311	–	5.306	$4.893 \pm 0.24\%$	92.2	1.68	34.54 ± 0.19
9	1060	1.492	3.990	5.324	$4.857 \pm 0.18\%$	91.2	1.56	34.29 ± 0.18
10	1090	1.422	4.472	5.347	$4.901 \pm 0.25\%$	91.7	1.60	34.59 ± 0.19
11	1120	1.686	2.186	5.413	$4.889 \pm 0.28\%$	90.3	1.56	34.51 ± 0.20
12	1150	2.266	19.822	5.564	$4.870 \pm 0.28\%$	87.5	1.33	34.38 ± 0.20
13	1200	3.139	0.271	5.841	$4.887 \pm 0.29\%$	83.7	1.02	34.50 ± 0.20
14	1250	14.382	32.293	9.138	$4.866 \pm 0.99\%$	53.2	0.26	34.35 ± 0.38

$\lambda = 5.543 \times 10^{-10} \text{ a}^{-1}$; sensitivity $\sim 7 \times 10^{-17} \text{ mol mV}^{-1}$; $^{40}\text{Ar}^*$ – radiogenic argon; $^{39}\text{Ar}_K$ – K-derived ^{39}Ar .
 $(^{36}\text{Ar}/^{37}\text{Ar})_{\text{Ca}} = 3.50 \times 10^{-4}$; $(^{39}\text{Ar}/^{37}\text{Ar})_{\text{Ca}} = 7.86 \times 10^{-4}$; $(^{40}\text{Ar}/^{39}\text{Ar})_K = 0.0249$ (99-250); 0.0257 (99-251).

Irradiation for 144 hours in X33 or X34, HIFAR reactor.

Fluence monitor: 92-716 sanidine from Fish Canyon Tuff; K–Ar reference age = 28.1 Ma.

Incremental total fusion age = 34.28 ± 0.21 Ma (99-250); 34.51 ± 0.19 Ma (99-251).

Weighted mean plateau age = 34.28 ± 0.18 Ma (99-250, steps 3 to 15); 34.47 ± 0.17 Ma (99-251, steps 2 to 14).

Isochron age, 99-250: 34.46 ± 0.25 Ma; MSWD = 1.78; $(^{40}\text{Ar}/^{36}\text{Ar})_i = 287.4 \pm 4.1$.

Isochron age, 99-251: 34.48 ± 0.28 Ma; MSWD = 2.53; $(^{40}\text{Ar}/^{36}\text{Ar})_i = 294.4 \pm 4.0$.

mean plateau age of 27.04 ± 0.14 Ma. The same data on an isochron diagram yield an indistinguishable age (Table 5). These results are entirely in agreement with the earlier K–Ar data and provide compelling evidence for a Late Oligocene eruption and cooling age for the Langaria Formation of 26.9 ± 0.2 Ma.

The Gum Dura Formation overlies the Bakate Formation in the Asille Group (Fig. 2) and, like the Langaria Formation, is formed predominantly of pantelleritic (rhyolitic) ignimbrites. Exposures of the Gum Dura ignimbrites do not occur in the Nabwal Hills but are found in the Irile Valley, and the upper Bakate Valley (Buluk Gap) to the south. We were able to sample an ignimbrite (99-242) from the Middle Member of the Gum Dura Formation from the Bakate Valley adjacent to the road to Buluk Wells. Total fusion ages on ten alkali feldspar single crystals provide a concordant data set with mean age of 15.85 ± 0.12 Ma (Table 4). Step heating of the alkali feldspar (Table 5) showed a relatively flat age spectrum, except for a higher age

for the initial step (Fig. 7). The plateau, incorporating over 98 % of the released argon, provides a weighted mean age of 15.85 ± 0.08 Ma. An isochron age of 15.79 ± 0.15 Ma is also derived from the step heating data (Table 5). Again the concordance of all the results at 15.8 ± 0.1 Ma, and the flat age spectrum, give confidence that the age relates to the cooling of this ignimbrite. These new ^{40}Ar – ^{39}Ar measurements are consistent and concordant with the earlier K–Ar ages of 15.8 ± 0.2 Ma from two units of the Middle Member of the Gum Dura Formation from sites about 4 km to the north (McDougall & Watkins, 1985), and from a sample in the Upper Member at a location near Langaria Gorge, about 35 km to the NNW (McDougall & Watkins, 1988).

The new results obtained from alkali feldspars from three ignimbrite units in the Asille Group are consistent with the stratigraphic order, and provide unambiguous evidence that in each case a precise and accurate age has been obtained for the eruption and cooling.

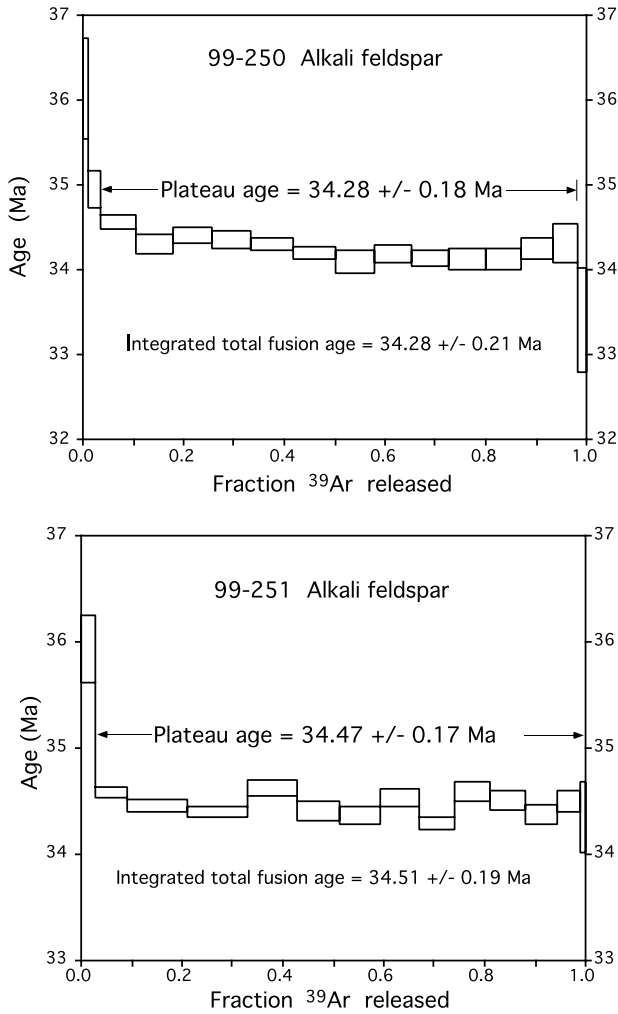


Figure 5. Age spectra for alkali feldspars from the ignimbrite in the Nabwal Formation. Width of age boxes reflect one standard deviation either side of the measured age.

5.b.2. Basalts of the Nabwal Formation

The Nabwal Formation (R. T. Watkins, unpub. Ph.D. thesis, Univ. London, 1983; Key & Watkins, 1988) consists predominantly of aphyric lavas of transitional basaltic composition. The true thickness of the lava succession is uncertain, owing to difficulty in gauging the extent of downthrow on several normal faults affecting the largely monotonous sequence. A minimum thickness of about 500 m, recorded during the initial reconnaissance study (R. T. Watkins, unpub. Ph.D. thesis, Univ. London, 1983) has been confirmed by re-measurement during the most recent investigations. The lowermost part of the formation is characterized by relatively thick lava flows that exhibit well-developed columnar jointing where exposed in the walls of river gorges. Appreciable weathering and palaeosol development are observed only locally in exposures of the lavas of the lower half of the sequence, and are extensive only within the upper 100 m or so of the formation. This may suggest that the lava pile was built quite

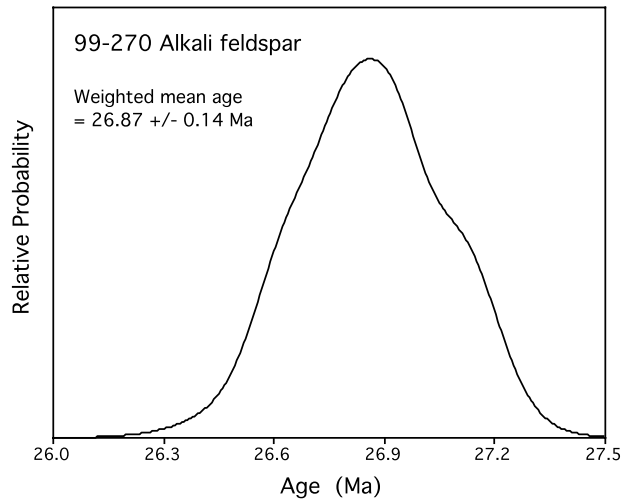


Figure 6. Probability plot of total fusion age data from single crystals of alkali feldspar from an ignimbrite (99-270) in the Langaria Formation.

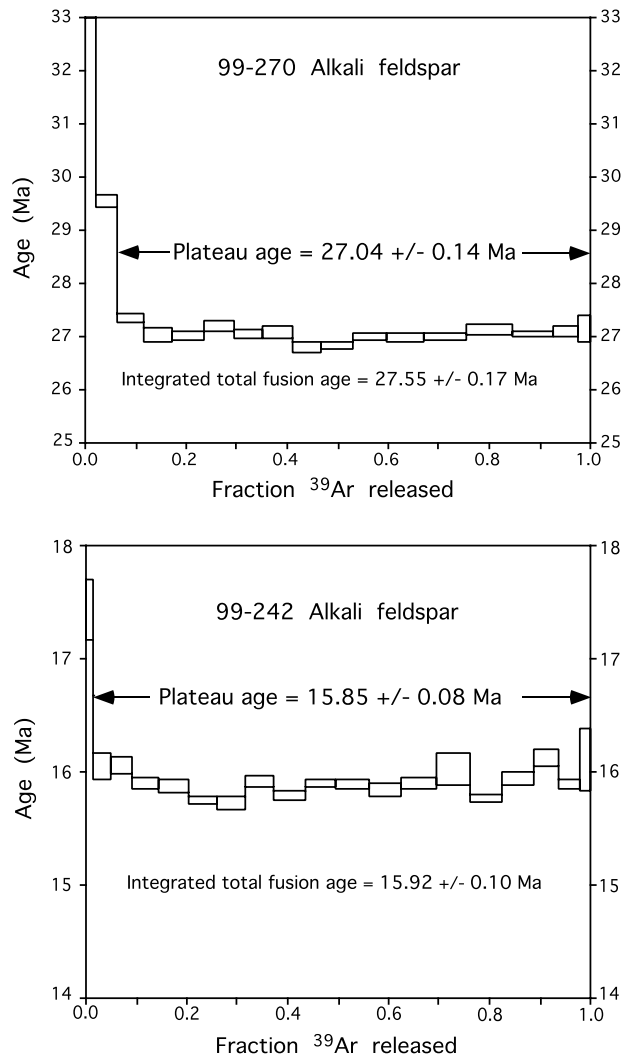


Figure 7. Age spectra for alkali feldspars separated from ignimbrite (99-270) in the Langaria Formation and from ignimbrite (99-242) in the Gum Dura Formation.

Table 4. Results of laser fusion ^{40}Ar – ^{39}Ar dating of single crystals of alkali feldspar from two ignimbrites from the Asille Group in the Il Bakate – Buluk Wells area, east of Koobi Fora and Lake Turkana, northern Kenya

Sample	$^{36}\text{Ar}/^{39}\text{Ar}$ $\times 10^{-5}$	$^{37}\text{Ar}/^{39}\text{Ar}$ $\times 10^{-4}$	$^{40}\text{Ar}/^{39}\text{Ar}$	$^{40}\text{Ar}^*/^{39}\text{Ar}_K$ \pm c.v.	% $^{40}\text{Ar}^*$	^{39}Ar 10^{-15} mol	Calculated age Ma \pm 1 s.d.
<i>99-242 ignimbrite, adjacent to road to Buluk Wells, Middle Member, Gum Dura Formation;</i>							
<i>4° 09.99'N 36° 35.42'E; J = 3.8381E-03 \pm 0.50%; level 3, ANU 59</i>							
1	21.04	28.47	2.372	2.286 \pm 0.74 %	96.4	10.7	15.76 \pm 0.14
2	0.440	1.427	2.342	2.316 \pm 0.40 %	98.9	5.8	15.97 \pm 0.10
3	1.880	0.898	2.347	2.317 \pm 0.34 %	98.7	9.2	15.97 \pm 0.10
4	2.592	0.749	2.326	2.294 \pm 0.54 %	98.6	11.0	15.82 \pm 0.12
5	22.00	17.80	2.398	2.308 \pm 0.33 %	96.3	9.7	15.91 \pm 0.09
6	0.515	31.72	2.334	2.308 \pm 0.51 %	98.9	7.4	15.91 \pm 0.11
7	6.981	44.39	2.322	2.278 \pm 0.43 %	98.1	5.3	15.70 \pm 0.10
8	4.394	1.049	2.359	2.322 \pm 0.45 %	98.4	7.9	16.00 \pm 0.11
10	8.709	23.30	2.325	2.275 \pm 0.32 %	97.8	7.9	15.69 \pm 0.09
11	26.20	39.46	2.384	2.282 \pm 0.45 %	95.7	6.3	15.73 \pm 0.10
Arithmetic mean age (n = 10)							15.85 \pm 0.12
<i>99-270 ignimbrite, pink, Il Irile, just south of Il Dura, Langaria Formation;</i>							
<i>4° 24.34'N, 36° 32.57'E; J = 4.007E-03 \pm 0.50%; level 7, ANU 59</i>							
1	5.914	5.351	3.791	3.747 \pm 0.28 %	98.8	10.5	26.88 \pm 0.15
2	8.268	54.74	3.806	3.756 \pm 0.26 %	98.7	6.5	26.95 \pm 0.15
3	11.45	179.8	3.832	3.774 \pm 0.58 %	98.5	2.4	27.07 \pm 0.21
4	14.89	1.198	3.802	3.732 \pm 0.26 %	98.2	7.5	26.77 \pm 0.15
5	28.17	51.36	3.839	3.730 \pm 0.74 %	97.2	4.9	26.76 \pm 0.24
6	17.13	41.51	3.823	3.747 \pm 0.75 %	98.0	5.6	26.88 \pm 0.24
7	21.86	6.047	3.838	3.747 \pm 0.47 %	97.6	7.0	26.88 \pm 0.18
8	15.37	13.33	3.813	3.741 \pm 0.31 %	98.1	9.7	26.84 \pm 0.16
9	27.82	28.57	3.820	3.712 \pm 0.32 %	97.2	5.6	26.63 \pm 0.16
10	42.33	73.56	3.892	3.742 \pm 0.63 %	96.1	4.0	26.85 \pm 0.21
11	17.28	13.67	3.793	3.716 \pm 0.38 %	98.0	8.7	26.66 \pm 0.17
12	10.09	12.21	3.837	3.781 \pm 0.36 %	98.5	7.2	27.13 \pm 0.17
13	40.48	376.3	3.920	3.779 \pm 0.32 %	96.4	4.9	27.11 \pm 0.16
14	56.00	170.8	3.899	3.709 \pm 0.69 %	95.1	3.9	26.61 \pm 0.23
Arithmetic mean age (n = 14)							26.86 \pm 0.17

$\lambda = 5.543 \times 10^{-10} \text{a}^{-1}$; sensitivity $\sim 2.6 \times 10^{-17} \text{mol/mV}^{-1}$.

$(^{36}\text{Ar}/^{37}\text{Ar})_{\text{Ca}} = 3.50 \times 10^{-4}$; $(^{39}\text{Ar}/^{37}\text{Ar})_{\text{Ca}} = 7.86 \times 10^{-4}$; $(^{40}\text{Ar}/^{39}\text{Ar})_{\text{K}} = 0.0246$ (99-242), 0.0262 (99-270).

$^{40}\text{Ar}^*$ – radiogenic ^{40}Ar ; $^{39}\text{Ar}_K$ – K-derived ^{39}Ar ; quoted error for each age includes estimated error in J.

Irradiation for 144 hours in X33 or X34, HIFAR reactor.

Fluence monitor: 92-176 sanidine from Fish Canyon Tuff; K–Ar reference age: 28.1 Ma.

rapidly by a series of basalt eruptions of significant magnitude. The Nabwal Formation basalts lie directly and unconformably on basement metamorphic rocks (Fig. 3), which show minimal weathering and soil development at the contact.

Potassium–argon ages on whole rock basalts from the lowermost formation of the Asille Group are listed in Table 1, arranged as far as possible in stratigraphic order. The measured ages range from 34.8 to 27.6 Ma, disregarding several anomalous younger apparent ages, not reported here as the calculated ages are younger than the overlying Langaria Formation whose age is well established.

Sample 99-267 is from a lava lying directly upon the metamorphic basement. Samples 99-263B and 99-258 are from lavas 0.6 and 1.3 km west of the metamorphic outcrop, and thus slightly higher in the succession than 99-267 (Fig. 3). Uncertainties in the scale of faulting between the sampling sites prevents more detailed appraisal of the stratigraphic relations. Samples 99-267 and 99-263B yield K–Ar ages of 33.5 ± 0.4 Ma and 34.8 ± 0.4 Ma, respectively, quite similar in age to the alkali feldspars dated from the rhyolitic ignimbrite, believed to be stratigraphically higher in the Nabwal

Formation. The substantially younger calculated K–Ar age of 27.6 ± 0.3 Ma for sample 99-258 is interpreted as reflecting significant loss of radiogenic argon.

A further three basalt samples give K–Ar ages ranging from 30.7 to 29.8 Ma (Table 1), each regarded as a minimum age only because of the significant proportion of mesostasis or partly altered glass in each sample. Sample 95-211, which yielded an age of 30.1 ± 0.3 Ma, was collected from a lava in the same fault block but stratigraphically lower than the rhyolitic ignimbrite that is dated at 34.3 ± 0.2 Ma. Thus, considerable loss of radiogenic argon, resulting in a younger apparent age, is clearly implicated in this case. The whole rock K–Ar ages of 28.2 ± 0.7 Ma and 26.8 ± 0.5 Ma on basalts from the Nabwal Formation, reported by Fitch *et al.* (1985), also are regarded as unrealistically young on the same grounds.

The results obtained in this study show that the lava eruptions of the Nabwal Formation began at least 34.8 ± 0.4 Ma ago in the Late Eocene. The duration of volcanism comprising the Nabwal Formation cannot be directly estimated from our new age data owing to their variability and apparent loss of radiogenic argon, leading to young apparent ages. However, our

Table 5. Results of ^{40}Ar - ^{39}Ar step heating experiments on alkali feldspar separated from an ignimbrite (99-270) in the Langaria Formation, Irile near Il Dura, Nabwal Hills, and from an ignimbrite (99-242) of the Middle Member of the Gum Dura Formation on the road to Buluk Wells, northern Kenya, $4^{\circ}24.34'\text{N}$, $36^{\circ}32.57'\text{E}$ and $4^{\circ}09.99'\text{N}$, $36^{\circ}35.42'\text{E}$, respectively

Step no.	Temp. °C	$^{36}\text{Ar}/^{39}\text{Ar}$ $\times 10^{-4}$	$^{37}\text{Ar}/^{39}\text{Ar}$ $\times 10^{-3}$	$^{40}\text{Ar}/^{39}\text{Ar}$	$^{40}\text{Ar}^*/^{39}\text{Ar}_K$ \pm c.v.	% $^{40}\text{Ar}^*$	^{39}Ar 10^{-14} mol	Calculated age Ma \pm 1 s.d.
<i>99-270 alkali feldspar, J = 4.007E-03 \pm 0.5%; level 7, ANU 59, 4.4 mg</i>								
1	750	29.974	33.667	7.449	6.540 \pm 0.29%	87.8	0.55	46.67 \pm 0.27
2	850	9.404	2.479	4.426	4.122 \pm 0.36%	93.1	1.24	29.55 \pm 0.18
3	900	6.881	11.682	4.041	3.813 \pm 0.28%	94.4	1.41	27.35 \pm 0.16
4	940	6.622	2.044	3.990	3.768 \pm 0.45%	94.4	1.65	27.03 \pm 0.18
5	970	6.664	2.510	3.990	3.767 \pm 0.32%	94.4	1.76	27.03 \pm 0.16
6	990	6.924	0.188	4.022	3.791 \pm 0.38%	94.3	1.63	27.19 \pm 0.17
7	1010	8.193	7.660	4.037	3.770 \pm 0.28%	93.4	1.60	27.04 \pm 0.15
8	1030	7.765	4.780	4.031	3.776 \pm 0.39%	93.7	1.60	27.09 \pm 0.17
9	1050	9.344	2.033	4.038	3.736 \pm 0.37%	92.5	1.61	26.81 \pm 0.17
10	1075	8.101	4.418	4.006	3.741 \pm 0.28%	93.4	1.74	26.84 \pm 0.15
11	1100	7.371	1.258	4.006	3.762 \pm 0.27%	93.9	1.88	26.99 \pm 0.15
12	1125	8.035	0.913	4.024	3.761 \pm 0.29%	93.5	2.07	26.98 \pm 0.15
13	1150	10.870	2.361	4.112	3.765 \pm 0.27%	91.6	2.37	27.01 \pm 0.15
14	1170	7.749	–	4.039	3.783 \pm 0.34%	93.7	2.48	27.14 \pm 0.16
15	1190	10.582	2.780	4.108	3.769 \pm 0.17%	91.8	2.25	27.04 \pm 0.14
16	1210	18.406	–	4.348	3.778 \pm 0.37%	86.9	1.44	27.10 \pm 0.17
17	1250	48.901	–	5.255	3.784 \pm 0.94%	72.0	0.66	27.15 \pm 0.29
18	1300	313.73	42.935	12.754	3.462 \pm 1.93%	27.1	0.15	24.85 \pm 0.49
<i>99-242 alkali feldspar, J = 3.838E-3 \pm 0.5%; level 3, ANU59, 5.7 mg</i>								
1	750	147.96	9.234	6.926	2.530 \pm 1.53%	36.5	0.61	17.43 \pm 0.28
2	850	48.248	–	3.779	2.329 \pm 0.76%	61.6	1.51	16.05 \pm 0.14
3	900	26.723	2.332	3.144	2.330 \pm 0.49%	74.1	1.83	16.06 \pm 0.11
4	940	14.119	1.949	2.748	2.306 \pm 0.30%	83.9	2.26	15.90 \pm 0.09
5	970	9.373	2.896	2.604	2.303 \pm 0.38%	88.4	2.48	15.87 \pm 0.10
6	990	7.771	0.310	2.539	2.284 \pm 0.18%	90.0	2.39	15.75 \pm 0.08
7	1010	7.263	1.337	2.520	2.281 \pm 0.37%	90.5	2.41	15.73 \pm 0.10
8	1030	5.843	–	2.506	2.308 \pm 0.33%	92.1	2.49	15.91 \pm 0.09
9	1050	6.116	4.157	2.495	2.291 \pm 0.28%	91.8	2.61	15.79 \pm 0.09
10	1070	5.950	–	2.506	2.306 \pm 0.22%	92.0	2.69	15.89 \pm 0.09
11	1090	6.327	3.259	2.516	2.305 \pm 0.27%	91.6	2.74	15.89 \pm 0.09
12	1110	5.304	–	2.480	2.299 \pm 0.38%	92.7	2.82	15.85 \pm 0.10
13	1130	5.472	–	2.492	2.306 \pm 0.31%	92.5	2.89	15.90 \pm 0.09
14	1150	5.821	–	2.522	2.326 \pm 0.89%	92.2	2.88	16.03 \pm 0.16
15	1170	7.749	–	2.540	2.286 \pm 0.22%	90.0	2.80	15.76 \pm 0.09
16	1190	8.543	–	2.589	2.312 \pm 0.35%	89.3	2.57	15.94 \pm 0.10
17	1210	11.468	0.497	2.703	2.339 \pm 0.43%	86.6	2.14	16.12 \pm 0.10
18	1250	18.301	1.517	2.871	2.306 \pm 0.29%	80.3	1.90	15.89 \pm 0.09
19	1300	57.124	–	4.049	2.337 \pm 1.67%	57.7	0.83	16.11 \pm 0.28

$\lambda = 5.543 \times 10^{-10} \text{ a}^{-1}$; sensitivity $\sim 3 \times 10^{-17} \text{ mol mV}^{-1}$; $^{40}\text{Ar}^*$ – radiogenic argon; $^{39}\text{Ar}_K$ – K-derived ^{39}Ar .
 $(^{36}\text{Ar}/^{37}\text{Ar})_{\text{Ca}} = 3.50 \times 10^{-4}$; $(^{39}\text{Ar}/^{37}\text{Ar})_{\text{Ca}} = 7.86 \times 10^{-4}$; $(^{40}\text{Ar}/^{39}\text{Ar})_K = 0.0262$ (99-270); 0.0246 (99-242).
 Irradiation for 144 hours in X33 or X34, HIFAR reactor.

Fluence monitor: 92-176 Sanidine from Fish Canyon Tuff; K-Ar reference age = 28.1 Ma.

Incremental total fusion age = 27.55 \pm 0.17 Ma (99-270); 15.92 \pm 0.10 Ma (99-242).

Weighted mean plateau age = 27.04 \pm 0.14 Ma (99-270, steps 3 to 17); 15.85 \pm 0.08 Ma (99-242, steps 2 to 19).

Isochron age, 99-270: 27.01 \pm 0.24 Ma; MSWD = 2.79; $(^{40}\text{Ar}/^{36}\text{Ar})_i = 299.8 \pm 11.8$.

Isochron age, 99-242: 15.79 \pm 0.15 Ma; MSWD = 3.26; $(^{40}\text{Ar}/^{36}\text{Ar})_i = 306.0 \pm 5.0$.

concordant results on the overlying Langaria Formation show that the Nabwal Formation extended to no younger than 26.9 \pm 0.2 Ma, in Oligocene times.

In southern Ethiopia, just to the north of the border with Kenya, Davidson (1983) defined the Fejej Formation to include basaltic lavas overlying the metamorphic basement. Davidson & Rex (1980) and Davidson (1983) reported a whole rock K–Ar age of 32.8 \pm 2.0 Ma for one of the basalt lavas exposed less than 15 km north of the border with Kenya. Asfaw *et al.* (1991) provided a K–Ar age of 34.2 \pm 0.6 Ma on a whole rock basalt of the Fejej Formation from near the Fejej police post, about 18 km north of the border. Davidson (1983) states that he regards the Fejej

Formation basalts as equivalent to those of the Nabwal Formation. The age data are entirely consistent with this view.

5.b.3. Basalts overlying the Nabwal Hills and Irile fossil sites

Fluviatile sediments, about 20 m thick, are the source of vertebrate bones at both the Irile and Nabwal Hills fossil sites. At Irile, sediments are exposed over < 1 km². In the Nabwal Hills, sediments crop out over about 7 km², preserved in a graben or half graben (Fig. 3). Here the sediments appear to have been deposited disconformably on a topography developed on the Nabwal Formation basalts, as at 4° 25.68' N,

36° 35.69' E, lavas of the Nabwal Formation crop out on a conical hill that rises 20 m above the sediments.

At both the Nabwal Hills and Irile fossil sites, the sediments are clearly overlain, essentially conformably, by strongly plagioclase–phyric basalts. These lava flows range from a few to 10 m in thickness and are commonly separated by rubbly flow-tops and well-formed palaeosols. At the Irile fossil site, these petrographically distinctive lavas and deeply weathered lava flows characterize the type section of the Irile Member of the Bakate Formation. In the vicinity of the Nabwal Hills site, however, several lava flows of similar plagioclase–phyric basalt overlying sedimentary units were initially included in the Nabwal Formation (R. T. Watkins, unpub. Ph.D. thesis, Univ. London, 1983), primarily on account of the absence of the intervening ignimbrites of the Langaria Formation in the reconnaissance traverse of the Nabwal Hills.

The results of K–Ar dating of lavas overlying the sediments at both the Nabwal Hills and Irile fossil sites are listed in Table 1. The plagioclase phenocrysts were in such abundance and of large enough size (often > 5 mm) to facilitate their separation. Samples of the basalts themselves were sufficiently fresh in petrographic thin-section to be regarded as suitable for dating as whole rock samples, although the presence of variably crystallized and at least slightly altered mesostasis was a concern in virtually all samples.

At Irile, sample 99-269 was collected from a gently rising hillside forming the southern margin of the sedimentary outcrop and represents the second lava flow above the fossiliferous sediments. The measured K–Ar ages of the plagioclase separate and of the whole rock, with very different potassium contents, are quite similar at 16.5 ± 0.2 Ma and 17.2 ± 0.2 Ma, respectively. The next flow in the sequence, sample 99-268, in contrast, yielded highly discordant apparent ages of 19.7 ± 0.3 Ma for the plagioclase, and 15.1 ± 0.2 Ma for the whole rock. Although plausible explanations can be advanced for these discordancies, such as argon loss from the groundmass of the whole rock and the presence of excess argon in the plagioclase, we prefer to state that an approximate age of 17 ± 2 Ma, the mean and standard deviation of the four measurements in Table 1, is indicated from our results.

The K–Ar age results from separated plagioclase and whole rock samples of basalt lavas overlying fossiliferous sediments at the Nabwal Hills site similarly show a good deal of scatter from 16.0 ± 0.2 to 20.6 ± 0.2 Ma (Table 1). Only one sample (99-272) shows concordant ages from the separated plagioclase and whole rock at 16.1 ± 0.2 Ma. The spread in apparent ages is much greater than experimental error and indicates failure of the samples to meet the assumptions underlying the K–Ar dating system. Hence, little is to be gained in attempting to justify or explain individual measured ages. A simple mean of the results yields an age estimate

of 17.4 ± 1.6 Ma, indistinguishable from the poorly constrained age for the Irile Member basalts at the Irile fossil site. Overall we conclude that the petrographically similar basalt lavas overlying the sediments at the Irile and Nabwal Hills fossil sites are of broadly equivalent age at approximately 17 ± 2 Ma, Early Miocene, providing a younger age limit for the sediments and the fauna contained therein. A maximum age limit for the sediments at the Irile site is 26.9 Ma, the age of the underlying Langaria Formation. At the Nabwal Hills site, we interpret the geology as indicating that the sediments are lying disconformably upon a topography developed upon the Nabwal Formation lavas, with the inference that the ignimbrites of the Langaria Formation did not extend to the eastern Nabwal Hills or, more probably, that they were eroded from this location, a broad river valley, prior to accumulation of the fossil-bearing sediments. On the basis of petrographic similarity and distinctiveness, and the age data, we interpret the basalt lava flows overlying the sediments at the Nabwal Hills fossil site as belonging to the Irile Member of the Bakate Formation.

The vertebrate fauna recovered from the Irile and Nabwal Hills sites appears similar and comparable to that at the Buluk fossil locality (J. G. Fleagle & J. M. Harris, pers. comm.). Buluk is located about 20 km to the south of the Nabwal Hills, and the sediments exposed there are included within the Buluk Member of the Bakate Formation (Watkins, 1989). The Buluk Member consists of fluvial sediments and reworked rhyolitic tuffs sandwiched between basalt lavas of the Irile Member beneath and the overlying II Jimma Member. The vertebrate fauna, which includes hominoids, has been described by Harris & Watkins (1974) and Leakey & Walker (1985). K–Ar ages on alkali feldspar from the tuffs and plagioclase from underlying basalt lavas gave ages in the range 16.1 to 17.2 Ma, Early Miocene (McDougall & Watkins, 1985). Thus, the ages derived for Irile and Nabwal Hills fossil sites are essentially concordant with the Buluk site ages, and support the correlation of the sedimentary units at Irile and Nabwal Hills with that exposed at Buluk. Also noteworthy is that at site FJ-18 on the Fejej Plain, about 3 km north of the Kenya–Ethiopia border, and approximately north of the Nabwal Hills fossil site, Tiffney, Fleagle & Bown (1994) and Richmond *et al.* (1998) reported the presence of plant and vertebrate fossils in sediments that they assigned to the Bakate Formation. The fauna is considered to be comparable to that at Buluk and a plagioclase–porphyritic basalt overlying the sediments yielded a well-defined whole rock ^{40}Ar – ^{39}Ar plateau age of 16.2 ± 0.1 Ma (Richmond *et al.* 1998), which is in keeping with this. Thus, it appears that Early Miocene sediments of broadly equivalent age are preserved in relatively small pockets, in some cases in downfaulted

blocks, over a significant area in northern Kenya and southern Ethiopia.

6. Conclusions

The metamorphic basement gneisses exposed in the eastern Nabwal Hills exhibit typical Pan-African cooling ages of 510 and 522 Ma, as recorded in biotite. In this region we have no further recorded history until the Palaeogene. Strata of the Asille Group, comprising a sequence more than 1400 m thick, is heavily faulted and exhibits a regional dip of about 6° to the SSW. The Nabwal Formation, consisting almost entirely of near-aphyric basalt lava flows, lies unconformably upon metamorphic basement and represents the initial phase of volcanism at this locality within the East African Rift System. Eruptions began approximately 35 Ma ago, Late Eocene, and accompanied early crustal extension prior to initiation of rifting. Davidson (1983) argued that in southern Ethiopia the early basaltic volcanics were erupted onto a landscape of low relief, and that major faulting and development of rift valleys occurred subsequent to much of the volcanism. This agrees with what is seen in the Nabwal Hills, noting, however, that major rifting was occurring simultaneously with the eruption of the Nabwal lavas only 90 km to the SSW with formation and filling of the Lokichar Basin half graben (Morley *et al.* 1992, 1999).

The Asille Group extends to younger than 13 Ma, the age of the Gurro Member of the Nakwele Formation (McDougall & Watkins, 1988), noting that at least 200 m of basaltic lava flows conformably overlie the ignimbrites of the Gurro Member (Fig. 3). Thus, rocks of the Asille Group were erupted over an interval exceeding 20 Ma.

Useful comparison can be made between the volcanic history recorded in the Nabwal Hills and in the Amaro Horst, 120 km to the NNE (Fig. 1). In the Amaro Horst, the lowermost flood basalts overlie crystalline metamorphic basement with age measurements indicating that the volcanism occurred between 45 and 35 Ma ago (WoldeGabriel *et al.* 1991; Ebinger *et al.* 1993; George, Rogers & Kelley, 1998). The Nabwal Formation basalts have comparable age to the Gamo basalt in the Amaro Horst with reported ages of 35 to 40 Ma. Initiation of volcanism, and crustal extension, in the Nabwal Hills appear therefore to have occurred up to 10 Ma later than at Amaro, consistent with the findings of George, Rogers & Kelley (1998) that commencement of volcanic activity becomes younger southwards.

Alkali feldspars from the Amaro rhyolitic tuff, conformably overlying the Gamo basalt, yielded ^{40}Ar – ^{39}Ar ages of 36.9 ± 0.2 Ma (Ebinger *et al.* 1993). These ages are slightly older than that of 34.3 ± 0.2 Ma recorded in this study for the thin ignimbrite within the Nabwal Formation, and illustrate that the production

of rhyolitic magma and the bimodal nature of the volcanism have been features of the rift evolution since earliest times.

In the Amaro Horst, following a long hiatus, a second pulse of flood basalt eruption occurred between 18 and 11 Ma ago (WoldeGabriel *et al.* 1991; Ebinger *et al.* 1993; George, Rogers & Kelley, 1998). Again, we find a parallel history in the Asille Group of the Nabwal Hills, with the Bakate and Nakwele formations, consisting predominantly of basaltic lavas, erupted over an equivalent time interval (Fig. 2). Thus, there appears to be a closely comparable history of volcanism in the Amaro Horst in the southern Ethiopian Rift and in the Nabwal Hills horst in the Kenya Rift, presumably reflecting similar tectonic processes operating throughout this segment of the East African Rift System.

In the Nabwal Hills, as throughout the wider Suregei-Asille uplands, it is clear that the major faulting and regional SSW tilting of the strata took place after 13 Ma ago, the maximum age for the youngest units of the Asille Group in this area, and before eruption of the essentially flat-lying basalts of the Gombe Group that began perhaps as early as 6 Ma ago (Fitch *et al.* 1985; McDougall & Watkins, 1988), but which occurred over extensive areas in the Turkana Basin between 4.2 and 3.9 Ma ago (Haileab *et al.* 2004). Thus, major tectonic development of the Chew Bahir and Lake Turkana grabens and the intervening Suregei-Asille horst probably occurred within an interval between sometime after 13 Ma and before 5 Ma, in Late Miocene times.

Acknowledgements. Fieldwork was supported by an Australian Research Council grant to R. T. Watkins. We thank the Government of Kenya and the National Museums of Kenya for their helpful cooperation. Neutron irradiations were facilitated by the Australian Institute of Nuclear Science and Engineering and the Australian Nuclear Science and Technology Organization. Technical assistance in the geochronology laboratories at the Australian National University was ably provided by R. Maier, X. Zhang and J. Mya. We thank N. Rogers and R. Macdonald for helpful reviews of the manuscript. Clementine Krayshek assisted in the drafting of the maps.

References

- ASFAW, B., BEYENE, Y., SEMAW, S., SUWA, G., WHITE, T. & WOLDEGABRIEL, G. 1991. Fejej: a new paleoanthropological research area in Ethiopia. *Journal of Human Evolution* **21**, 137–43.
- BERGGREN, W. A., KENT, D. V., SWISHER III, C. C. & AUBRY, M.-P. 1995. A revised Cenozoic geochronology and chronostratigraphy. In *Geochronology, Time Scales and Stratigraphic Correlation* (eds W. A. Berggren, D. V. Kent, D.-V. Aubry and J. Hardenbol), pp. 129–212. Tulsa: Society for Sedimentary Geology (SEPM), Special Publication no. 54.

- CAHEN, L. & SNELLING, N. J. 1966. *The Geochronology of Equatorial Africa*. Amsterdam: North-Holland, 195 pp.
- CHU, D. & GORDON, R. G. 1999. Evidence for motion between Nubia and Somalia along the Southwest Indian ridge. *Nature* **398**, 64–7.
- DAVIDSON, A. 1983. The Omo River Project. Reconnaissance geology and geochemistry of parts of Ilubabor, Kefa, Gemu Gofa and Sidamo, Ethiopia. *Ethiopian Institute of Geological Surveys, Bulletin* **2**, 89 pp.
- DAVIDSON, A. & REX, D. C. 1980. Age of volcanism and rifting in southwestern Ethiopia. *Nature* **283**, 657–8.
- DEMETTS, C., GORDON, R. G., ARGUS, D. F. & STEIN, S. 1990. Current plate motions. *Geophysical Journal International* **101**, 425–78.
- DEMETTS, C., GORDON, R. G., ARGUS, D. F. & STEIN, S. 1994. Effect of recent revisions to the geomagnetic reversal time scale on estimates of current plate motions. *Geophysical Research Letters* **21**, 2191–4.
- EBINGER, C. J., BECHTEL, T. D., FORSYTH, D. W. & BOWIN, C. O. 1989. Effective elastic plate thickness beneath the East African and Afar Plateaus and dynamic compensation of the uplifts. *Journal of Geophysical Research* **94**, 2883–901.
- EBINGER, C. J., YEMANE, T., HARDING, D. J., TESFAYE, S., KELLEY, S. & REX, D. C. 2000. Rift deflection, migration, and propagation: Linkage of the Ethiopian and Eastern rifts, Africa. *Geological Society of America Bulletin* **112**, 163–76.
- EBINGER, C. J., YEMANE, T., WOLDEGABRIEL, G., ARONSON, J. L. & WALTER, R. C. 1993. Late Eocene–Recent volcanism and faulting in the southern main Ethiopian rift. *Journal of the Geological Society, London* **150**, 99–108.
- FERNANDES, R. M. S., AMBROSIUS, B. A. C., NOOMEN, R., BASTOS, L., COMBRINCK, L., MIRANDA, J. M. & SPAKMAN, W. 2004. Angular velocities of Nubia and Somalia from continuous GPS data: implications on present-day relative kinematics. *Earth and Planetary Science Letters* **222**, 197–208.
- FITCH, F. J., HOOKER, P. J., MILLER, J. A., MITCHELL, T. G. & WATKINS, R. T. 1985. Reconnaissance potassium–argon geochronology of the Suregei–Asille district, northern Kenya. *Geological Magazine* **122**, 609–22.
- FLEAGLE, J. G., BOWN, T. M., HARRIS, J. M., WATKINS, R. T. & LEAKEY, M. G. 1997. Fossil monkeys from Northern Kenya. (Abstract). *American Journal of Physical Anthropology, Supplement* **24**, 111.
- FLEAGLE, J. G., HARRIS, J. M., WATKINS, R. T. & MILLER, E. R. 2000. Early Miocene mammalian faunas from northern Kenya and southern Ethiopia. (Abstract). *Journal of Vertebrate Paleontology* **20**, Supplement no. 3, Abstract of Papers, p. 41A.
- FURMAN, T., BRYCE, J. G., KARSON, J. & IOTTI, A. 2004. East African Rift System (EARS) plume structure: Insights from Quaternary mafic lavas of Turkana, Kenya. *Journal of Petrology* **45**, 1069–88.
- GEORGE, R. M. & ROGERS, N. W. 2002. Plume dynamics beneath the African plate inferred from the geochemistry of the Tertiary basalts of southern Ethiopia. *Contributions to Mineralogy and Petrology* **144**, 286–304.
- GEORGE, R., ROGERS, N. & KELLEY, S. 1998. Earliest magmatism in Ethiopia: Evidence for two mantle plumes in one flood basalt province. *Geology* **26**, 923–6.
- HAILEAB, B., BROWN, F. H., MCDUGALL, I. & GATHOGO, P. N. 2004. Gombe Group basalts and initiation of Pliocene deposition in the Turkana depression, northern Kenya and southern Ethiopia. *Geological Magazine* **141**, 41–53.
- HARRIS, J. M. & WATKINS, R. T. 1974. New Early Miocene vertebrate locality near Lake Rudolf, Kenya. *Nature* **252**, 576–7.
- HENDRIE, D. B., KUSZNIR, N. J., MORLEY, C. K. & EBINGER, C. J. 1994. Cenozoic extension in northern Kenya: a quantitative model of rift basin development in the Turkana region. *Tectonophysics* **236**, 409–38.
- KEY, R. M. & WATKINS, R. T. 1988. Geology of the Sabarei area. *Mines and Geology Department, Ministry of Environment and Natural Resources, Nairobi, Kenya, Report* **111**, 57 pp.
- KRISP WORKING PARTY. 1991. Large-scale variation in lithospheric structure along and across the Kenya rift. *Nature* **354**, 223–7.
- LATIN, D., NORRY, M. J. & TARZEY, R. J. E. 1993. Magmatism in the Gregory Rift, East Africa: Evidence for melt generation by a plume. *Journal of Petrology* **34**, 1007–27.
- LEAKEY, M. G., FEIBEL, C. S., MCDUGALL, I., WARD, C. & WALKER, A. 1998. New specimens and confirmation of an early age for *Australopithecus anamensis*. *Nature* **393**, 62–6.
- LEAKEY, R. E. F. & WALKER, A. 1985. New higher primates from the early Miocene of Buluk, Kenya. *Nature* **318**, 173–5.
- MACDONALD, R., ROGERS, N. W., FITTON, J. G., BLACK, S. & SMITH, M. 2001. Plume–lithosphere interactions in the generation of the basalts of the Kenya Rift, East Africa. *Journal of Petrology* **42**, 877–900.
- MACDONALD, R., WILLIAMS, L. A. J. & GASS, I. G. 1994. Tectonomagmatic evolution of the Kenya rift valley: some geological perspectives. *Journal of the Geological Society, London* **151**, 879–88.
- MCDUGALL, I. & FEIBEL, C. S. 1999. Numerical age control for the Miocene–Pliocene succession at Lothagam, a hominoid-bearing sequence in the northern Kenya Rift. *Journal of the Geological Society, London* **156**, 731–45.
- MCDUGALL, I. & HARRISON, T. M. 1999. *Geochronology and Thermochronology by the $^{40}\text{Ar}/^{39}\text{Ar}$ Method*. 2nd ed. New York: Oxford University Press, 269 pp.
- MCDUGALL, I. & WATKINS, R. T. 1985. Age of hominoid-bearing sequence at Buluk, northern Kenya. *Nature* **318**, 175–8.
- MCDUGALL, I. & WATKINS, R. T. 1988. Potassium–argon ages of volcanic rocks from northeast of Lake Turkana, northern Kenya. *Geological Magazine* **125**, 15–23.
- MCKENZIE, D. P. & BICKLE, M. J. 1988. The volume and composition of melt generated by extension of the lithosphere. *Journal of Petrology* **29**, 625–79.
- MECHIE, J., KELLER, G. R., PRODEHL, C., GACIRI, S., BRAILE, L. W., MOONEY, W. D., GAJEWSKI, D. & SANDMEIER, K.-J. 1994. Crustal structure beneath the Kenya Rift from axial profile data. *Tectonophysics* **236**, 179–200.
- MOHR, P. 1983. Ethiopian flood basalt province. *Nature* **303**, 577–84.
- MOORE, J. M. & DAVIDSON, A. 1978. Rift structure of southern Ethiopia. *Tectonophysics* **46**, 159–73.
- MORLEY, C. K. (ed.) 1999. *Geoscience of Rift Systems – Evolution of East Africa*. American Association of Petroleum Geologists (AAPG), Studies in Geology vol. 44, 242 pp.
- MORLEY, C. K., NGENOH, D. K. & EGO, J. K. 1999. Introduction to the East African Rift System. In

- Geoscience of Rift Systems – Evolution of East Africa* (ed. C. K. Morley), pp. 1–18. AAPG Studies in Geology no. 44.
- MORLEY, C. K., WESCOTT, W. A., STONE, D. M., HARPER, R. M., WIGGER, S. T., DAY, R. A. & KARANJA, F. M. 1999. Geology and geophysics of the western Turkana basins, Kenya. In *Geoscience of Rift Systems – Evolution of East Africa* (ed. C. K. Morley), pp. 19–54. AAPG Studies in Geology, no. 44.
- MORLEY, C. K., WESCOTT, W. A., STONE, D. M., HARPER, R. M., WIGGER, S. T. & KARANJA, F. M. 1992. Tectonic evolution of the northern Kenya Rift. *Journal of the Geological Society, London* **149**, 333–48.
- RICHMOND, B. G., FLEAGLE, J. G., KAPPELMAN, J. & SWISHER III, C. C. 1998. First hominoid from the Miocene of Ethiopia and the evolution of the catarrhine elbow. *American Journal of Physical Anthropology* **105**, 257–77.
- ROGERS, N., MACDONALD, R., FITTON, J. G., GEORGE, R., SMITH, M. & BARREIRO, B. 2000. Two mantle plumes beneath the East African rift system; Sr, Nd and Pb isotope evidence from Kenya Rift basalts. *Earth and Planetary Science Letters* **176**, 387–400.
- SPELL, T. L. & MCDUGALL, I. 2003. Characterization and calibration of $^{40}\text{Ar}/^{39}\text{Ar}$ dating standards. *Chemical Geology* **198**, 189–211.
- SPELL, T. L., MCDUGALL, I. & DOULGERIS, A. P. 1996. Cerro Toledo Rhyolite, Jemez Volcanic Field, New Mexico: $^{40}\text{Ar}/^{39}\text{Ar}$ geochronology of eruptions between two caldera-forming events. *Geological Society of America Bulletin* **108**, 1549–66.
- STEIGER, R. H. & JÄGER, E. 1977. Subcommission on Geochronology: Convention on the use of decay constants in geo- and cosmochronology. *Earth and Planetary Science Letters* **36**, 359–62.
- STEWART, K. & ROGERS, N. 1996. Mantle plume and lithosphere contributions to basalts from southern Ethiopia. *Earth and Planetary Science Letters* **139**, 195–211.
- TIFFNEY, B. H., FLEAGLE, J. G. & BOWN, T. M. 1994. Early to Middle Miocene angiosperm fruits and seeds from Fejej, Ethiopia. *Tertiary Research* **15**, 25–42.
- WATKINS, R. T. 1986. Volcano-tectonic control on sedimentation in the Koobi Fora sedimentary basin, Lake Turkana. In *Sedimentation in the African Rifts* (eds L. E. Frostick, R. W. Renaut, I. Read and J. J. Tiercelin), pp. 85–94. Geological Society of London, Special Publication no. 25. Oxford: Blackwell Scientific Publications.
- WATKINS, R. T. 1989. The Buluk Member, a fossil hominoid-bearing sedimentary sequence of Miocene age from northern Kenya. *Journal of African Earth Sciences* **8**, 107–12.
- WOLDEGABRIEL, G., YEMANE, T., SUWA, G., WHITE, T. & ASEFAW, B. 1991. Age of volcanism and rifting in the Burgi-Soyoma area, Amaro Horst, southern Main Ethiopian Rift: geo- and biochronologic data. *Journal of African Earth Sciences* **13**, 437–47.

Copyright of Geological Magazine is the property of Cambridge University Press and its content may not be copied or emailed to multiple sites or posted to a listserv without the copyright holder's express written permission. However, users may print, download, or email articles for individual use.